Laser Performance and Investigation the Optimal Density Functional and the Dependence of the Basis Sets for (E, E)-2, 5-bis (3, 4-Dimethoxystyryl) Pyrazine (BDP) Molecule.

mahmoud sakr (mahmoud.sakr@must.edu.eg)
Misr University for Science and Technology https://orcid.org/0000-0001-8819-592X
Sayed Abdel Gawad
Misr University for Science and Technology
Samy Eldaly
Tanta University
Maram Abou Kana
Cairo University
El-Zeiny Ebeid
Tanta University

Research Article

Keywords: Sol-gel, Copolymer, Quantum dots (QDs), Laser behavior, photostability, Time dependent density function theory (TDDFT)

Posted Date: March 30th, 2021

DOI: https://doi.org/10.21203/rs.3.rs-353079/v1

Version of Record: A version of this preprint was published at Journal of Molecular Modeling on August 20th, 2021. See the published version at https://doi.org/10.1007/s00894-021-04876-0.

Abstract

This manuscript includes some photophysical parameters and some optical properties such as absorption and emission spectra of the (E, E)- 2,5-bis (3,4-dimethoxystyryl) pyrazine (BDP) by applying sol-gel and copolymer matrices. The BDP molecular structure is incorporated in sol-gel matrix and copolymer of methyl methacrylate (MMA) and 2-hydroxy metylmethacrylate (HEMA). In case of sol-gel matrix, the BDP molecular structure has higher quantum yield in addition to photostability maxima. The laser behavior of this molecular structure containing sol-gel matrix is good senior compared to copolymer one via using diode laser (450nm) as pumping laser of power 160 mW. Also, the fluorescence profile of the BDP molecular structure is sensitized via using cadmium sulphide (CdS) quantum dots (QDs) by applying sol-gel host. The optimized structure of the BDP molecule is obtained via applying B3LYP/6-31G(d) level of theory. The electronic absorption and emission spectra of the BDP molecular structure in ethanol solvent, were calculated using time dependent density functional theory (TDDFT) at CAM-B3LYP /6-31G++(d, p) level. The obtained theoretical results were compared to experimental ones.

1. Introduction

In our previous work, some photophysical parameters, laser performance, quantum dot photosensitization and TDDFT of (E, E)-2, 5-bis [2-(4-(dimethylamino)phenyl) ethenyl]pyrazine (BDPEP) molecular structure via applying sol-gel and copolymer matrices are studied (1). Consequently, the same previous studies for BDP molecular structure are investigated due to the different chemical structure of BDP molecule compared to BDPEP molecular structure.

As of a late, a great deal of a work is presented to actualize laser dyes via applying solid-state as a useful option in contrast to the partner of liquid dye lasers owing to their compactness, ease of manufacture, low cost of fabrication, simplicity and wellbeing in taking care of and activity. In addition to, avoiding lack of toxicity, flammability, flow fluctuations, and solvent evaporation problems (2-4). A lot of laser dyes via applying solid hosts have been broadly announced (5-16). In solid-state dye lasers (SDDL) (17), the day is interacted with matrix through a hydrogen bonds among the dye and hydroxyls. This allow the dye to be adsorbed on the surface of the matrix. Thereby, preventing the dye bimolecular reactions and upgrade the dye thermal and environmental stability (18, 19).

In a prior investigation, we detailed the laser activity and optical behavior of the BDP laser dyes in organic solvents (20). Hence, the study the performance of this laser dye via applying sol–gel matrix and copolymer media is essential to upgrade the nature of laser action. The existence of HEMA kept up the transparency of solid matrix as well as ensured a good solubility of probe dye because of the polar character of HEMA (21, 22). In the preparation of copolymer (MMA and HEMA), azobisisobutyronitrile (AIBN) was used as a initiator for free radical bulk polymerization of HEMA and MMA. The optical properties and lasing action of the BDP molecule via applying sol-gel and copolymer matrices are assessed.

Organic particles with huge delocalised л-electron systems along their back bone have attracted significant interest because of potential applications related with strong emission behavior and enormous nonlinear optical properties (23-25). The electron-donating and electron-withdrawing groups play important roles in the optical properties of organic compounds (26). The six-membered ring that contain nitrogen atoms at the 1, 4 positions is called pyrazines (26, 27). Being of their highly electron-withdrawing character, pyrazine compounds are perfect for the incorporation as electron-withdrawing groups in favoring intramolecular charge transfer (ICT) (26).

Quantum dots (QDs) have a large potential uses as photosensitizers for a verity of application. Upon resizing the QDs, the electronic absorption and emission spectra of it can be adjusted. Studies recording the factors controlling the potential energy transfer process among donor molecule (QD) and acceptor molecules are investigated (28).

2. Material And Methods

2.1 Materials preparation

2.1.1 The BDP molecule preparation (29)**.** In dimethylformamide (DMF), the mixture from 2,5-dimethylpyrazine(0.5g, 0.00462 M) and 3,4-dimethoxybenzaldhyde (2.3g, 0.013 M) were dissolved and the mixture were cooled to 0.0 ^{o}C (scheme 1). Then, potassium-tert-butanolate (1.55g, 13mM) was added with small amount to this mixture and brought to ambient temperature. Via applying stirrer, the mixture was stirred till completely consumed. By extraction with chloroform, the product was isolated after the completion the reaction. The product material obtained was recrystalizased to give (1.4g, 52%) as a yellow solid. The structure of the compound was assured via applying ^{1}H NMR and ^{13}C NMR.

2.1.2 The preparation sol-gel matrix containing the BDP molecule (30)**.** The sol-gel matrix was prepared as follows (Scheme 2); via applying the magnetic stirrer, we mix (11.00 mL tetraethoxysilan (TEOS) (Aldrich, 98%), 6.00 mL methanol (Aldrich), 9.00 mL distilled water, one mL of hydrochloric acid (HCl) (Merck, approximately 35% pure, 1.18 gm^{-1}) (0.1N) as a catalyst and 8.00 mL glycerol (Merck, IP for analysis) as a drying control chemical (DCCA) for 6 hours at 60 ° C. In polystyrene cuvette, 1.00 mL of the BDP solution is mixed with 3.00 mL sol. It was dehydrated and aging for about three weeks via applying a controlled oven at 60 ° C.

2.1.3 The preparation of sol-gel matrix containing CdS QDs (31). In order to prepare QDs in the silica matrix, QDs should be synthesized in aqueous rather than organic medium. As the solubility of aqueous QDs in sol-gel is excellent compared to organic QDs. Thus, CdS QDs in aqueous media is prepared as follows; 250 mL three-necked flask. In this flask, we mixed 100 mL $CdCl_2$ (0.02M), 2.5mL H_2O, then under stirring, 1.0 mL from thioglycolic acid was added. The PH was fixed to 12.00 via using 1.00 M NaOH. Then, 0.3mL of 30% H_2O_2 drop wisely added in the flask after moving the solution for 10 minutes.

2.1.4 The preparation of copolymer (MMA/ HEMA) containing BDP molecule (32)**:** The copolymer of methymethacrylate (MMA) and hydroxylethylmethacrylate (HEMA) was prepared via mixing MMA and HEMA (volume ratio 2:1) monomers containing the initiator azobisisobutyronitrile (AIBN) 3g/L dissolved in it. Then, the prepared solution was subjected to ultrasonic stirring for about 15 minute until the initiator was completely dissolved. After that, the BDP solution was added to obtain the desired concentration and allowed to dissolve in the ultrasonic bath for up to 20 minute. In controlled clean oven at 60^{o}C as an optimum temperature regarding physical appearance and transparency, drying and aging were carried out. After one week from the date of preparation, the samples got dried so they could be handled and subjected to various measurements.

2.2 Characterization: Via applying a transmission electron microscope (TEM) with acceleration voltage up to 200 kV, the morphology and the size of the CdS QDs were recorded. Utilizing UV-vis spectrophotometer (Shimadzu UV-2450), the optical properties of the BDP molecule are measured over a range of 200-700 nm. The fluorescence properties were measured via utilizing spectrofluorometer (Shimadzu, RF-5301PC).

3. Results And Discussion

The electronic absorption and emission spectra of the studied molecule was measured experimentally via applying sol-gel and copolymer matrices; the results are presented in Fig. 1. The electronic absorption spectrum of the studied molecular structure in sol-gel and copolymer matrices consists of mainly one peak appearing at 374 and 409nm respectively. It is assigned as π-π* transition as indicated by its extinction coefficient, 8280 and 7250 $Lmol^{-1}cm^{-1}$ for the studied molecule via applying sol-gel and copolymer matrices respectively. On the other hand, the electronic emission spectra of the studied system were also recorded by applying sol-gel and copolymer matrices and presented in Fig. 1. The experimental maximum emission wavelength of the BDP molecular structure in sol-gel and copolymer matrices is 502 and 485 nm respectively. As presented in Fig. 1, the interference among the experimental electronic absorption and emission spectra were not observed by applying sol-gel contrast to copolymer one. Therefore, the reabsorption of the experimental electronic emission photons of the studied molecular structure has not been occurred by applying sol-gel matrix contrast to copolymer host as presented in Fig. 1.

Via utilizing Fig. 1, the fluorescence quantum yield (f_f) (33, 34), oscillator strength ( ), transition dipole moment from ground to excited state (μ_{12}) (35-37), radiative decay rate constant (K_r) (38) for the studied molecule by applying sol-gel and copolymer matrices are estimated and presented in Table 1. The f_f value of the studied molecule by applying sol-gel matrix is high contrast to copolymer matrix as listed in Table 1. Owing to high mobility of the BDP molecules in sol-gel compared to copolymer host. In addition to, the highest value of K_r of the BDP molecule embedded sol-gel matrix contrast to copolymer one as shown in Table 1. Referring to, the high singlet- triplet splitting energies ($\Delta E_{S,T}$) of the studied molecular structure by applying sol-gel matrix compared to the copolymer host (39-42). The value of *f* and μ_{12} of

the studied molecule via applying sol-gel and copolymer matrices indicating (S_0 S_1 electronic transition).

Table 1: Photo physical parameters of BDP molecule by applying sol-gel and copolymer matrices.

Hosts	$\lambda_{abs.}$ (nm)	$\lambda_{ems.}$ (nm)	f_f		$K_r \times 10^9$ (S^{-1})	μ_{12} (Debay)
sol-gel	374	502	0.52	0.82	0.85	9.63
copolymer	409	485	0.43	0.62	0.79	8.62

The experimental overlapping between electronic absorption spectrum of the studied molecule and emission spectrum the CdS QDs by applying sol-gel matrix was examined; the results are given in Fig. 2a. Via applying the following equations (43),

$$D=(1.6122\times10^{-9})\lambda^4-(2.6575\times10^{-6})\lambda^3+(1.6242\times10^{-3})\lambda^2-(0.4277)\lambda+(41.57),$$

$\varepsilon = 587(D)^{2.65}$, where D (nm) is the size of the nanocrystal administration sample, λ (nm) is the wavelength and is the molar absorptivity of the first excitonic absorption peak of the corresponding sample. The used molar concentration of the synthesized CdS QDs was 6.6×10^{-6} M and the CdS QDs size was 3-6 nm. The CdS QDs TEM image is shown in Fig. 2b.

Due to large overlapping between emission spectrum of the CdS QDs and absorption spectrum of the studied molecule by applying sol-gel matrix as presented in Fig. 2a. The emission spectrum of the studied molecule was upgraded in sol-gel matrix via adding different concentrations of CdS QDs as shown in Fig. 3. The experimental electronic maximum fluorescence intensity at 503nm is enhanced subsequently and the position of the electronic maximum emission wavelength at 503nm is not influenced as shown in (Fig. 3). This refers to, the fluorescence emission of the studied molecule in sol-gel matrix is photosensitized via applying different concentration of CdS QDs.

Assuming the photo-stability of the sample is defined as the time needed to reduce the energy output intensity to half of its value. Hence, the half-life time of the BDP molecular structure embedded sol-gel and copolymer matrices is 70 and 50 minutes respectively as shown in Fig 4A using a 450nm wavelength diode laser and a power of 160 mW as a source of pumping. Consequently, the half-life time of the BDP molecular structure via applying sol-gel matrix is higher than that copolymer because the mobility of the BDP molecules in sol-gel matrix is higher than that in copolymer.

Supposing that the amplified spontaneous emission (ASE) efficiency is defined as the ratio between the output energy of the target molecule over arrange of input pumping energy (44). Hence, the ASE (a.u.) efficiency of 1×10^{-3} M BDP molecule via applying sol-gel matrix is higher than that in copolymer as given in Fig.4B. Which indicates, the highest number of excited BDP molecules in sol-gel matrix contrast to

copolymer one. Via utilizing diode laser of 450nm wavelength, the input energy was controlled and varied between 160 to 300 mW.

The electronic ground state structures of the studied compounds were obtained utilizing the density functional theory (DFT) (45) method. The chemical structure optimizations were carried out at the B3LYP /6-31G(d) level of theory (46-48) and the results are given in Fig. 5. BDP molecular structure planar as presented in Fig. 5. The geometrical parameters of the BDP compound in gas state are listed in Table 2. The labeling scheme is recorded in Fig. 5. Table 2 showed some selected bond lengths and dihedral angles of the studied BDP molecular structure. From Table 2, some comments can be listed: (1) Referring to the listed dihedral angles, the two phenyl rings and the pyrazine ring together with the two vinyl groups all lie in the same plane. (2) The bond lengths of the two vinyl groups (C_{12}-C_{11} and C_8-C_7) are very slightly different (ca. 0.001 Å). (3) The two methyl groups that bind to O_{38} and O_{35} rotate by dihedral angle 110.78 and 108.97^o due to steric hindrance. (4) The obtained bond angles refers to the sp^2 hybridization over the entire molecular structure. (5) The changes in the obtained bond lengths as all carbon–carbon, ring's carbon-oxygen and ring's carbon–nitrogen bonds are either doubly bonded or partially multiply bonded.

Table 2: Selected optimized geometrical parameters (bond length in Å and dihedral angle in ^{o}) computed for BDP molecule in gas phase using B3LYP/6-31G(d). For labeling, refer to Fig. 5.

Dihedral angle (degree)	Designation	Bond length(A)	Designation
179.77	C_{47}-O_{37}-C_{25}-C_{26}	1.373	C_{26}-O_{38}
110.78	C_{51}-O_{38}-C_{26}-C_{22}	1.363	C_{25}-O_{37}
179.79	C_3-N_{33}-C_2-C_7	1.461	C_{23}-C_{12}
108.97	C_{39}-O_{35}-C_{18}-C_{29}	1.351	C_{12}-C_{11}
179.61	C_{43}-O_{36}-C_{17}-C_{18}	1.457	C_{11}-C_4
124.89	C_{16}-C_{17}-O_{36}	1.456	C_2-C_7
120.85	O_{35}-C_{18}-C_{17}	1.352	C_7-C_8
115.69	O_{37}-C_{25}-C_{26}	1.459	C_8-C_{19}
121.11	O_{38}-C_{26}-C_{25}	1.359	C_{17}-O_{36}
124.11	C_{12}-C_{11}-C_4	1.377	C_{18}-O_{35}

The graphical presentation of the HOMO / LUMO orbitals, energy gap between HOMO and LUMO (E_g) for BDP compound in gas at B3LYB/6-31G(d) level of theory is shown in Fig. 6. The л-bonding orbitals and the lone pairs of electrons of the oxygen atoms of the BDP molecule are delocalized over the whole BDP

molecule (see Fig. 6). In addition to, the л* anti-bonding orbitals in the LUMO energy level (see Fig. 6), are distribute over the whole of the BDP molecular structure. While, the four oxygen atoms in the BDP molecule have a small part in distribution over the whole molecule.

The optimal density functional and the dependence of the basis sets for BDP molecular structure are investigated in two steps; the results are presented in Figs (7 and 8). The first step; in which, the choice of the optimal dependence of the DFT functionals are studied (B3LYP (49), CAM-B3LYP (50), M06-2X (51), ωB97X-D (52) [42]) (53) as recorded in Fig. 7. The optimal DFT function for calculated electronic absorption spectra of the BDP molecular structure in ethanol is CAM-B3LYP (see Fig. 7). Via applying CAM-B3LYP function, the calculated electronic absorption spectrum of the BDP molecular structure is in agreement with the experimental results as recorded in Fig. 7.

The second step in which the dependence on the basis set is recorded via applying the CAM-B3LYP functional. The computational electronic absorption spectra of the BDP molecular structure in ethanol were studied by applying different basis sets; the results are given in Fig. 8. The diffuse functions must be used to obtain the more accurate electronic absorption results for BDP molecular structure in ethanol solvent as presented in Table 3. Therefore, the optical properties of the BDP molecular structure in ethanol are investigated via applying CAM-B3LYP functional with the 6-311++G (d, p) basis set.

Table 3: The calculated maximum absorption wavelength (Calc. λ_{abs}. (nm)) of the BDP in ethanol with the use of different basis sets and practical absorption wavelength (Exp. λ_{abs}. (nm)). The CAM-B3LYP functional was applied.

Basis sets	Calc. λ_{abs}. (nm)	Pract. λ_{abs}. (nm)
6-31G(d)	388	408
6-31G(d, p)	388	
6-31G+(d, p)	401	
6-31G++(d, p)	401	
6-311G	382	
6-311G(d, p)	395	
6-311G++(d, p)	406	

The calculated and experimental electronic absorption and emission spectra of the BDP molecule in ethanol are studied; the obtained spectra are presented in Fig. 9. The calculated electronic maximum absorption and emission wavelength of the BDP molecule is 406 and 508nm respectively as presented in Fig. 9. In addition to, the experimental maximum absorption and emission wavelength of the BDP molecule is 408 and 514nm respectively as presented in Fig. 9. Therefore, the computational calculated

absorption and emission spectra of the BDP molecule are in agreement with experimental results as recorded in Fig. 9.

From previous study and this study, the photophysical parameters, laser performance and QDs photosensitization of the BDPEP (1)and BDP molecular structures are upgraded by applying sol-gel matrix compared to copolymer. In addition to, the calculated optical properties of the BDPEP and BDP molecular structures are in agreement with experimental results using M06-2X/6-311G++(d,p) and CAM-B3LYP/6-311++(d,p) levels respectively.

Conclusions

The photophysical parameters such as fluorescence quantum yield (Φ_f), oscillator strength ( ), radiative decay rate constant (K_r), change dipole moment from ground to excited state (μ_{12}), gain coefficient and efficiency of the BDP molecule via applying sol-gel matrix are upgraded compared to copolymer. The mixing of CdS QDs to the BDP compound in sol-gel matrix is obtained successfully. The fluorescence emission of the BDP upon using sol-gel matrix is sensitized via adding different concentration of the CdS QDs. The lasing properties and photostability of the BDP molecule via applying sol–gel are recorded and compared to copolymer matrices. From these studies, we concluded that the Photodegradation rates for the BDP molecular structure via utilizing sol–gel matrix was generally lower than via using copolymer. The optical properties of the BDP molecule are calculated using the CAM-B3LYP functional with the 6-311++G (d, p) basis set. The computational calculated absorption and emission spectra of the BDP molecule are in agreement with experimental results.

Declarations

Code availability N/A

Author contribution

Mahmoud A.S. Sakr: Data curation, Methodology, Software. **Sayed A. Abdel Gawad**: Software, Validation. **Maram T.H. Abou Kana**: Visualization, Investigation. **Samy A. El-Daly**: Supervision. **El-Zeiny M. Ebeid**: Writing - review & editing.

Funding: This work was supported by Tanta University (Faculty of Science) and Cairo University (Laser Systems Department, National Institute of Laser- Enhanced Science (NILES).

Data availability All data generated or analysed during this study are included in this published article.

Declarations

Conflict of interest: The authors declare no competing interests

References

1. Sakr MAS, Abdel Gawad SA, El-Daly SA, Abou Kana MTH, Ebeid E-ZM. Photophysical and TDDFT investigation for (E, E)-2, 5-bis [2-(4-(dimethylamino)phenyl) ethenyl]pyrazine (BDPEP) laser dye in restricted matrices. Journal of Molecular Structure. 2020;1217:128403.
2. Susdorf T, Del Agua D, Tyagi A, Penzkofer A, Garcia O, Sastre R, et al. Photophysical characterization of pyrromethene 597 laser dye in silicon-containing organic matrices. Applied Physics B. 2007;86(3):537-45.
3. Garcia-Moreno I, Costela A, Martin V, Pintado-Sierra M, Sastre R. Materials for a Reliable Solid-State Dye Laser at the Red Spectral Edge. Advanced Functional Materials. 2009;19(16):2547-52.
4. Rong-Wei F, Yu-Gang J, Yuan-Qin X, De-Ying C. Enhanced laser characteristics of pyrromethene 650 using modified PMMA as solid hosts. Chinese Physics B. 2011;20(8):084205.
5. Sakr MA, Gawad SAA, Kana MTA, Ebeid E-ZM. Laser Performance of Some Oxazole Laser Dyes in Restricted Matrices. Journal of fluorescence. 2017;27(4):1267-75.
6. Somasundaram G, Ramalingam A. Gain studies of Coumarin 490 dye-doped polymer laser. Chemical Physics Letters. 2000;324(1-3):25-30.
7. Howell BF, Kuzyk MG. Amplified spontaneous emission and recoverable photodegradation in polymer doped with Disperse Orange 11. JOSA B. 2002;19(8):1790-3.
8. Bergmann A, Holzer W, Stark R, Gratz H, Penzkofer A, Amat-Guerri F, et al. Photophysical characterization of pyrromethene dyes in solid matrices of acrylic copolymers. Chemical Physics. 2001;271(1-2):201-13.
9. Giffin SM, McKinnie IT, Wadsworth WJ, Woolhouse AD, Smith GJ, Haskell TG. Solid state dye lasers based on 2-hydroxyethyl methacrylate and methyl methacrylate co-polymers. Optics communications. 1999;161(1-3):163-70.
10. Ahmad M, King TA, Ko D-K, Cha BH, Lee J. Photostability of lasers based on pyrromethene 567 in liquid and solid-state host media. Optics communications. 2002;203(3-6):327-34.
11. Amhad M, King T, Ko D-K, Cha BH, Lee J. Photostability of lasers based on pyrromethene 567 in liquid and solid-state host media. Optics Communications. 2002;203:327-34.
12. Costela A, García-Moreno I, Gómez C, Amat-Guerri F, Liras M, Sastre R. Efficient and highly photostable solid-state dye lasers based on modified dipyrromethene. BF 2 complexes incorporated into solid matrices of poly (methyl methacrylate). Applied physics B. 2003;76(4):365-9.
13. Costela A, García-Moreno I, Del Agua D, García O, Sastre R. Highly photostable solid-state dye lasers based on silicon-modified organic matrices. Journal of applied physics. 2007;101(7):073110.
14. Zhi H, Zhi-Yu W, Yu Y, Jun C, Min-Quan W, Cheng-Fang B, et al. Tunable solid-state dye laser with narrow linewidth operation. Chinese Physics Letters. 2001;18(2):225.
15. Yokoyama S, Nakahama T, Mashiko S. Amplified spontaneous emission and laser emission from a high optical-gain medium of dye-doped dendrimer. Journal of luminescence. 2005;111(4):285-90.
16. Russell JA, Pacheco DP, Russell WH, Aldag HR, Manenkov AA, editors. Laser threshold and efficiency measurements of solid state dye lasers operating in the near-infrared under microsecond pumping.

Solid State Lasers XI; 2002: International Society for Optics and Photonics.

17. Avnir D, Kaufman VR, Reisfeld R. Organic fluorescent dyes trapped in silica and silica-titania thin films by the sol-gel method. Photophysical, film and cage properties. Journal of non-crystalline solids. 1985;74(2-3):395-406.
18. Costa TM, Stefani V, Gallas MR, Balzaretti NM, da Jornada JA. Fluorescence properties of benzoxazole type dyes entrapped in a silica matrix by the sol–gel method. Journal of Materials Chemistry. 2001;11(12):3377-81.
19. Sakr MA, Gawad E-SAA, Kana MTA, Ebeid E-ZM. Photophysical, photochemical and laser behavior of some diolefinic laser dyes in sol–gel and methyl methacrylate/2-hydroxyethyl methacrylate copolymer matrices. Optics & Laser Technology. 2015;71:78-84.
20. El-Daly SA, Alamry KA. Spectroscopic Investigation and Photophysics of a D-π-A-π-D Type Styryl Pyrazine Derivative. Journal of fluorescence. 2016;26(1):163-76.
21. Costela A, Garcia-Moreno I, Figuera J, Amat-Guerri F, Sastre R. Polymeric matrices for lasing dyes: recent developments. Laser Chemistry. 1998;18(1-2):63-84.
22. Schafer FP. Dye lasers. 1990.
23. Kim HN, Guo Z, Zhu W, Yoon J, Tian H. Recent progress on polymer-based fluorescent and colorimetric chemosensors. Chemical Society Reviews. 2011;40(1):79-93.
24. He GS, Tan L-S, Zheng Q, Prasad PN. Multiphoton absorbing materials: molecular designs, characterizations, and applications. Chemical reviews. 2008;108(4):1245-330.
25. Li Z, Li Q, Qin J. Some new design strategies for second-order nonlinear optical polymers and dendrimers. Polymer Chemistry. 2011;2(12):2723-40.
26. Achelle S, Baudequin C, Plé N. Luminescent materials incorporating pyrazine or quinoxaline moieties. Dyes and Pigments. 2013;98(3):575-600.
27. Orešić M, Danilovski A, Dumić M, Košutić-Hulita N. One pot synthesis of 6, 12-dihydro-1, 3, 7, 9-tetramethyl-5H, 11H-dipyrido [1, 2-a: 1', 2'-d] pyrazine-2, 8-dione by hilbert-johnson reaction of 2-chloromethyl-3, 5-dimethyl-4-methoxypyridine. Journal of Heterocyclic Chemistry. 2001;38(3):785-90.
28. Talapin DV, Rogach AL, Mekis I, Haubold S, Kornowski A, Haase M, et al. Synthesis and surface modification of amino-stabilized CdSe, CdTe and InP nanocrystals. Colloids and Surfaces A: Physicochemical and Engineering Aspects. 2002;202(2-3):145-54.
29. Asiri AM, Alamry KA, Pannipara M, Al-Sehemi AG, El-Daly SA. Spectroscopic investigation, photophysical parameters and DFT calculations of 4, 4'-(1E, 1' E)-2, 2'-(pyrazine-2, 5-diyl) bis (ethene-2, 1-diyl) bis (N, N-dimethylaniline)(PENDA) in different solvents. Spectrochimica Acta Part A: Molecular and Biomolecular Spectroscopy. 2015;149:722-30.
30. Deshpande AV, Rane JR, Jathar LV. Comparison of spectroscopic and lasing properties of different types of sol-gel glass matrices containing Rh-6G. Journal of fluorescence. 2009;19(6):1083.

31. Yu WW, Qu L, Guo W, Peng X. Experimental determination of the extinction coefficient of CdTe, CdSe, and CdS nanocrystals. Chemistry of Materials. 2003;15(14):2854-60.
32. Macret M, Hild G. Hydroxyalkyl methacrylates: hydrogel formation based on the radical copolymerization of 2-hydroxyethylmethacrylate and 2, 3-dihydroxypropylmethacrylate. Polymer. 1982;23(5):748-53.
33. Kumar S, Rao V, Rastogi R. Excited-state dipole moments of some hydroxycoumarin dyes using an efficient solvatochromic method based on the solvent polarity parameter, ETN. Spectrochimica Acta Part A: Molecular and Biomolecular Spectroscopy. 2001;57(1):41-7.
34. Turki H, Abid S, El Gharbi R, Fery-Forgues S. Optical properties of new fluorescent iminocoumarins. Part 2. Solvatochromic study and comparison with the corresponding coumarin. Comptes Rendus Chimie. 2006;9(10):1252-9.
35. El-Daly SA, El-Azim SA, Elmekawey FM, Elbaradei BY, Shama SA, Asiri AM. Photophysical parameters, excitation energy transfer, and photoreactivity of 1, 4-bis (5-phenyl-2-oxazolyl) benzene (POPOP) laser dye. International Journal of Photoenergy. 2012;2012.
36. Katchalski-Katzir E, Haas E, Steinberg I. Study of conformation and intramolecular motility of polypeptides in solution by a novel fluorescence method. Annals of the New York Academy of Sciences. 1981;366(1):44-61.
37. Schneider C. Berichte der Bunsengesellschaft für Physikalische Chemie. Zeitschrift für Physikalische Chemie. 1967;54(5_6):332-3.
38. Fahmy HM, Kandel HM, Al-shamiri HA, Negm NA, Elwahy AH, Kana MTA. Spectroscopic Study of Solvent Polarity on the Optical and Photo-Physical Properties of Novel 9, 10-bis (coumarinyl) anthracene. Journal of fluorescence. 2018;28(6):1421-30.
39. Ebeid E-ZM, AlHazny SM. Photophysical and Laser-based Techniques in Chemistry, Biology and Medicine: Booksurge; 2006.
40. Bojinov V, Grabchev I. Synthesis and photophysical investigations of novel combined benzo [de] anthracen-7-one/2, 2, 6, 6-tetramethylpiperidines as fluorescent stabilisers for polymer materials. Polymer degradation and stability. 2004;85(2):789-97.
41. Yang Y, Wang M, Qian G, Wang Z, Fan X. Laser properties and photostabilities of laser dyes doped in ORMOSILs. Optical Materials. 2004;24(4):621-8.
42. Mula S, Ray AK, Banerjee M, Chaudhuri T, Dasgupta K, Chattopadhyay S. Design and development of a new pyrromethene dye with improved photostability and lasing efficiency: theoretical rationalization of photophysical and photochemical properties. The Journal of organic chemistry. 2008;73(6):2146-54.
43. Murillo AG, Calderon VHC, Romo FdJC, Velázquez DYM. F-127-Assisted Sol-Gel Synthesis of Gd2O3: Eu3+ Powders and Films. Materials Research. 2019;22(3).
44. Xu H. Nanophotonics: Manipulating Light with Plasmons: Pan Stanford; 2017.
45. Frisch M, Trucks GW, Schlegel HB, Scuseria GE, Robb MA, Cheeseman JR, et al. Gaussian~ 09 Revision D. 01. 2014.

46. Miehlich B, Savin A, Stoll H, Preuss H. Results obtained with the correlation energy density functionals of Becke and Lee, Yang and Parr. Chemical Physics Letters. 1989;157(3):200-6.
47. Lee SU. Influence of exchange-correlation functional in the calculations of vertical excitation energies of halogenated copper phthalocyanines using time-dependent density functional theory (TD-DFT). Bulletin of the Korean Chemical Society. 2013;34(8):2276-80.
48. Sun J, Li G, Liang W. How does the plasmonic enhancement of molecular absorption depend on the energy gap between molecular excitation and plasmon modes: A mixed TDDFT/FDTD investigation. Physical Chemistry Chemical Physics. 2015;17(26):16835-45.
49. Becke AD. Becke's three parameter hybrid method using the LYP correlation functional. J Chem Phys. 1993;98(492):5648-52.
50. Yanai T, Tew DP, Handy NC. A new hybrid exchange–correlation functional using the Coulomb-attenuating method (CAM-B3LYP). Chemical Physics Letters. 2004;393(1-3):51-7.
51. Zhao Y, Truhlar DG. The M06 suite of density functionals for main group thermochemistry, thermochemical kinetics, noncovalent interactions, excited states, and transition elements: two new functionals and systematic testing of four M06-class functionals and 12 other functionals. Theoretical Chemistry Accounts. 2008;120(1-3):215-41.
52. Chai J-D, Head-Gordon M. Long-range corrected hybrid density functionals with damped atom–atom dispersion corrections. Physical Chemistry Chemical Physics. 2008;10(44):6615-20.
53. Deshpande AV, Kumar U. Effect of method of preparation on photophysical properties of Rh-B impregnated sol–gel hosts. Journal of non-crystalline solids. 2002;306(2):149-59.

Figures

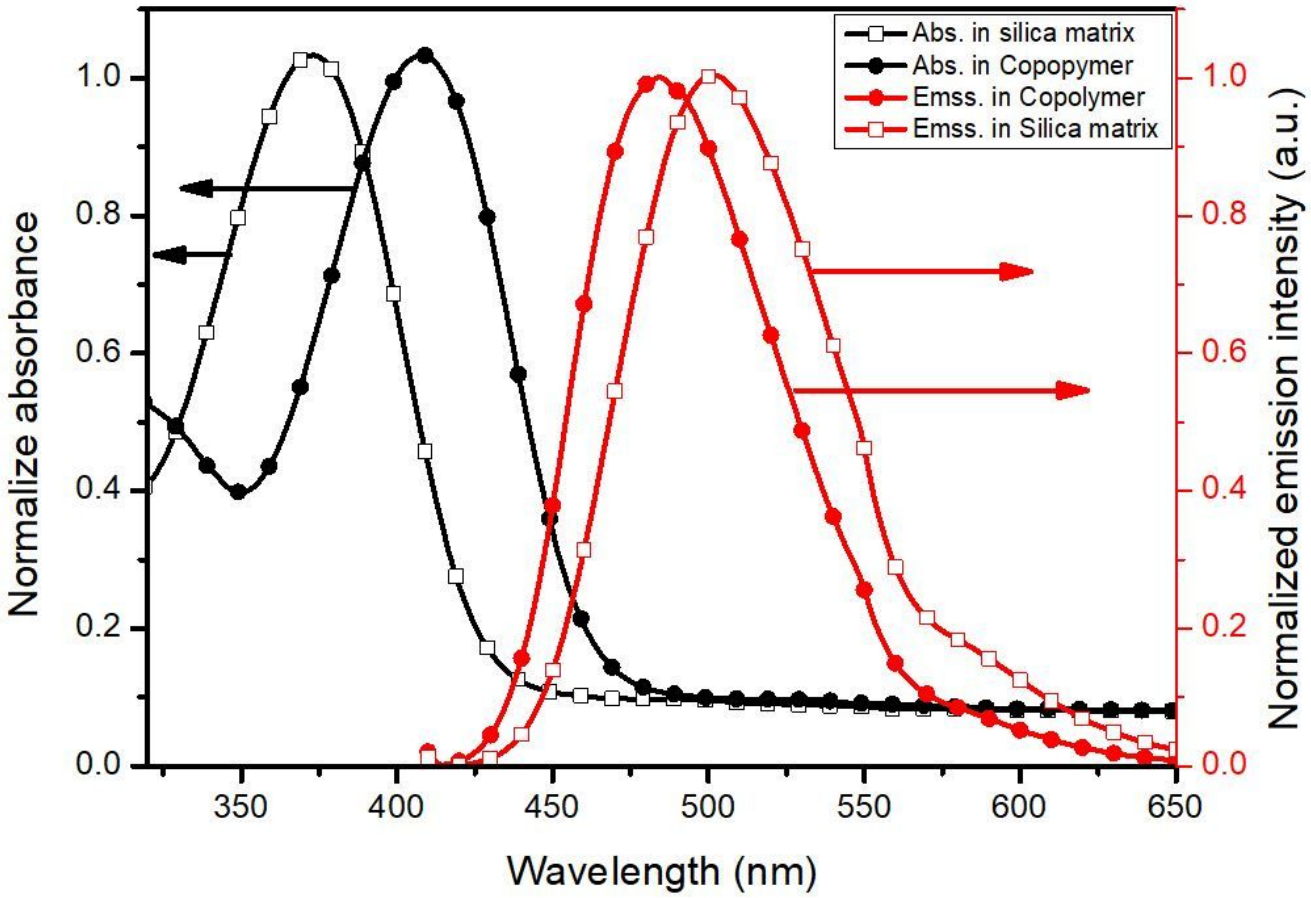

Figure 1

Normalized absorption (in black) and emission (in red) spectra of 1×10-5M BDP in sol-gel and copolymer matrices.

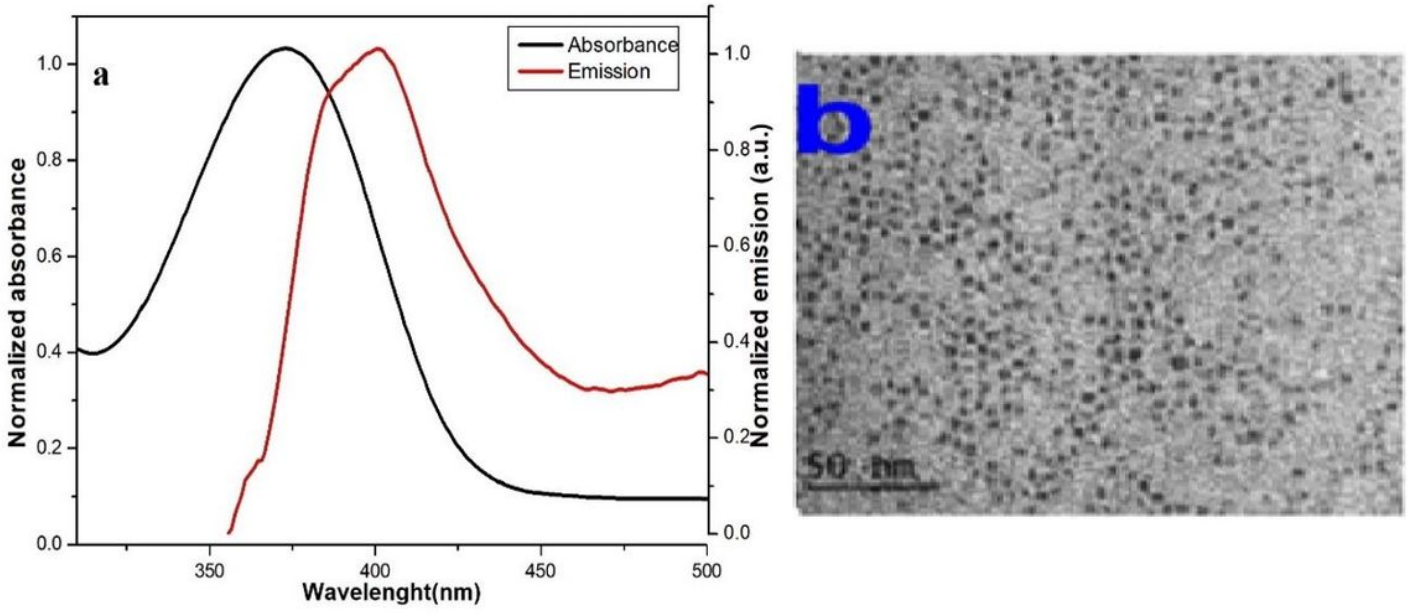

Figure 2

(a) The spectral overlaps of 1×10-5M of BDP absorption and6.6×10-6mol/L CdS QDs emission spectra (excitation wavelength λex.=380nm) in silica matrix. (b) The TEM image of CdS QDs.

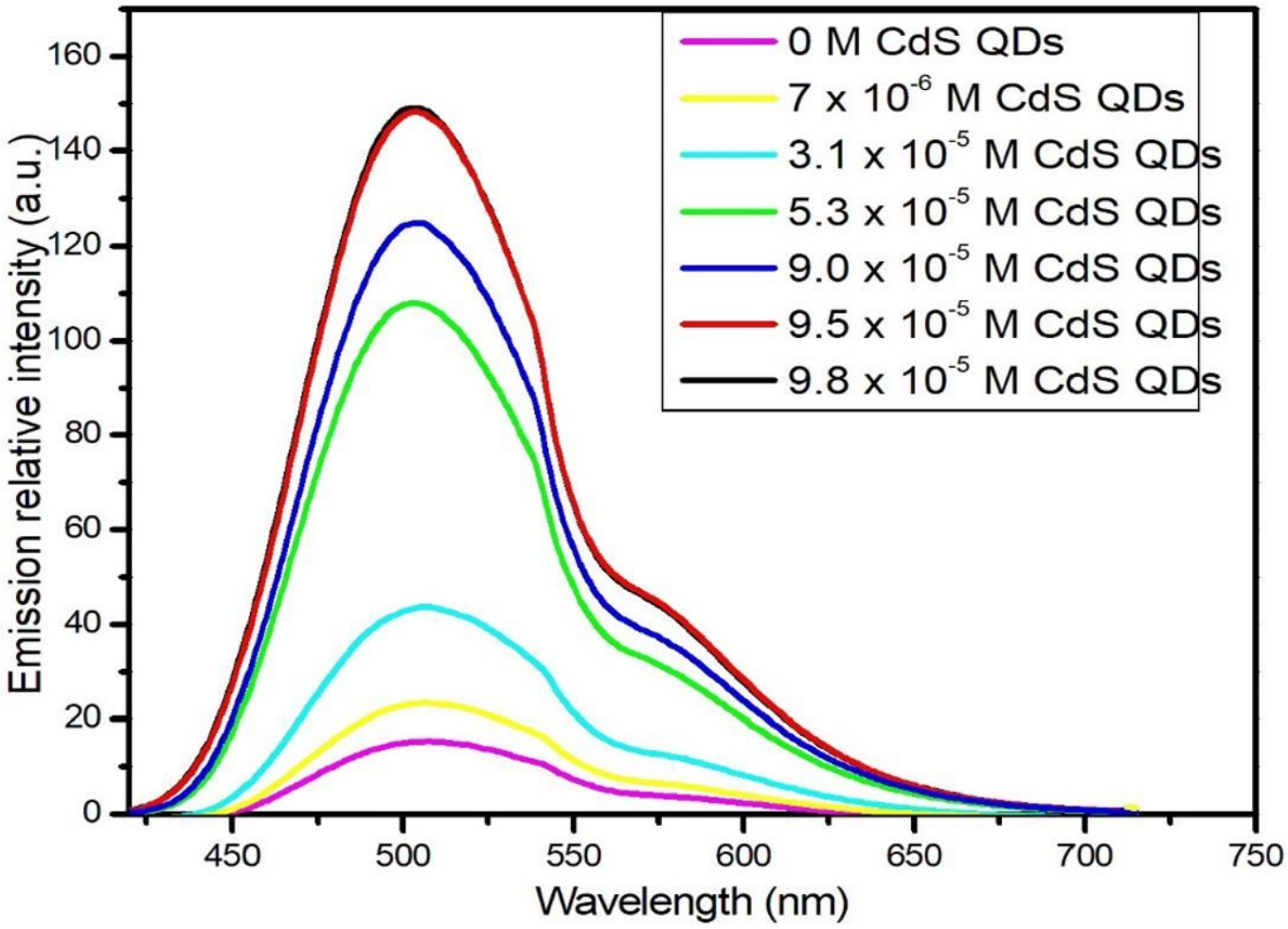

Figure 3

Emission spectra of 1×10-5M BDP dye in sol-gel matrix at different concentrations of CdS QDs (excitation wavelength (λex.=380 nm).

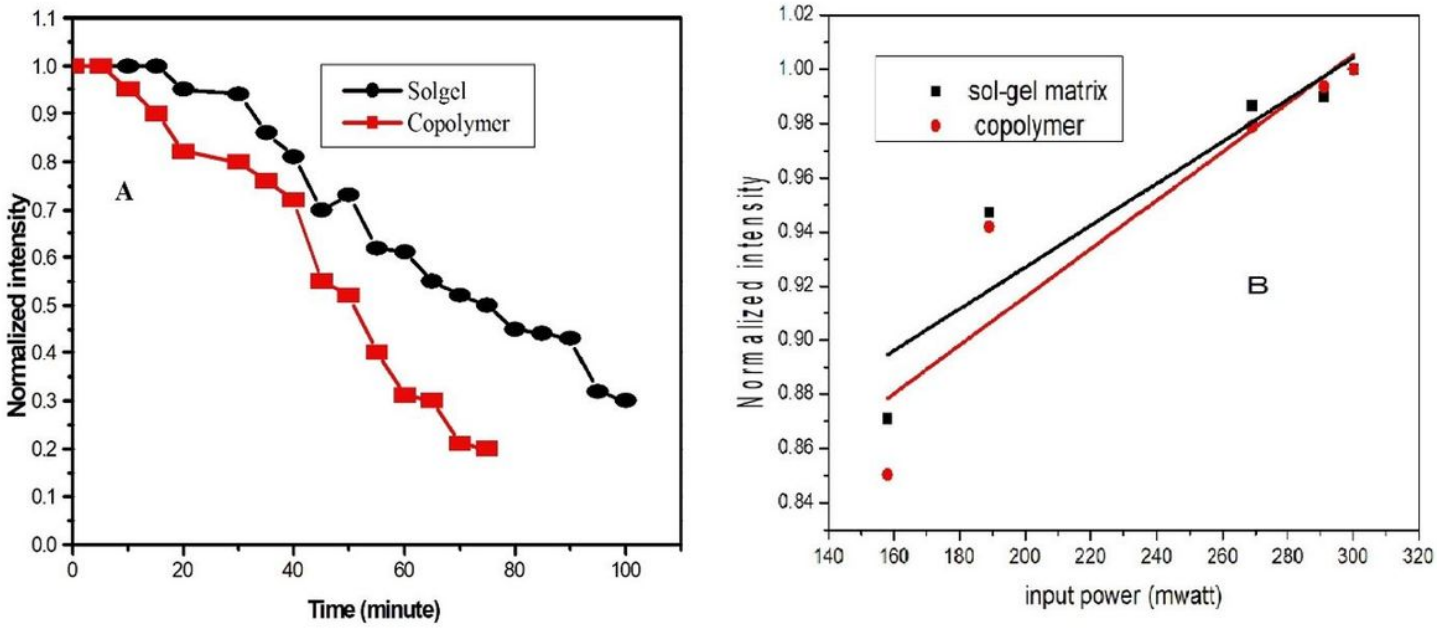

Figure 4

The output intensity as a function of time utilizing a 450nm wavelength diode laser and a power of 160 mW as a source of pumping (A) and the output intensity as a function of different input energy (B) for 1×10-3 M BDP dye by applying both sol-gel and copolymer matrices utilizing diode continuous laser (λ=450 nm).

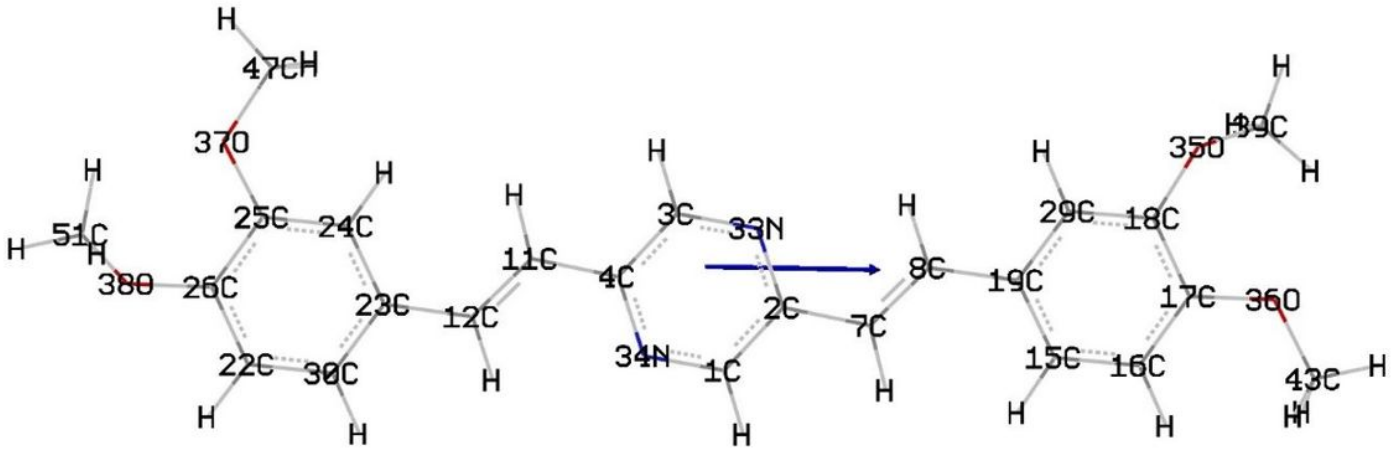

Figure 5

Optimized geom. of BDP compound.

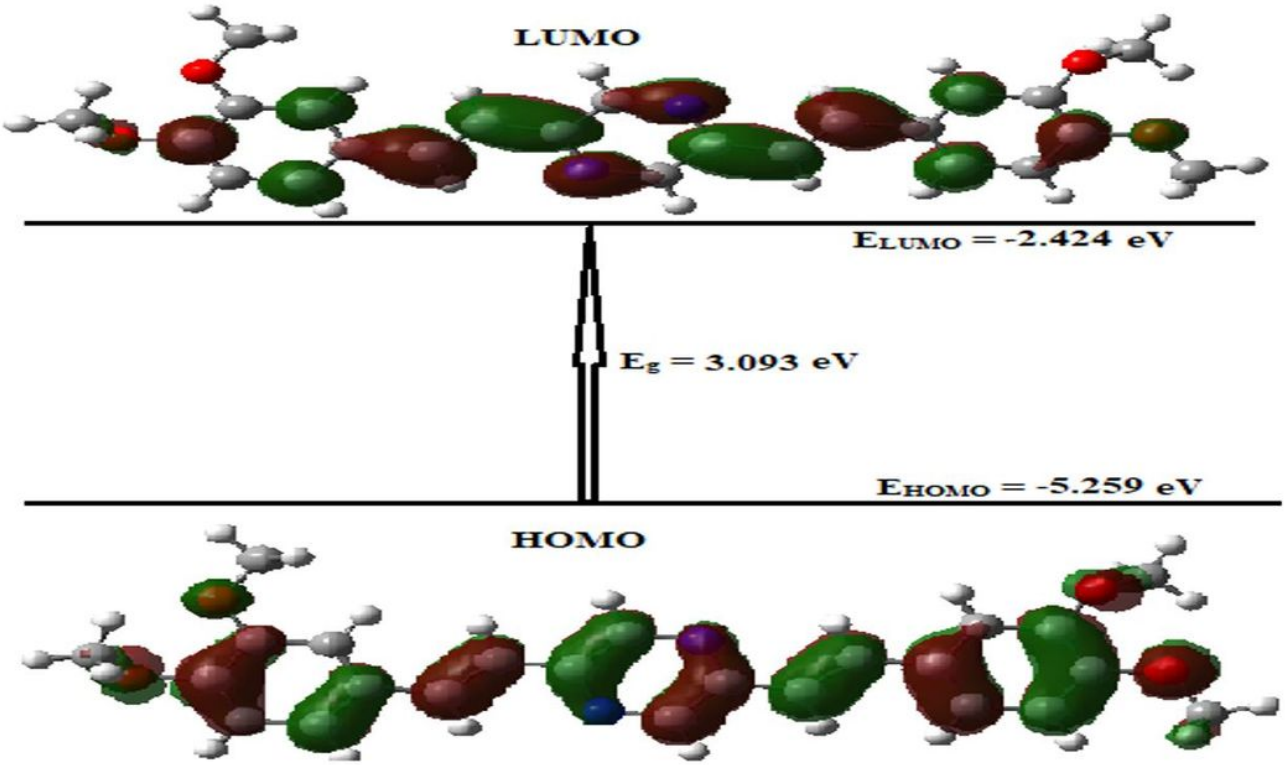

Figure 6

The graphical presentation of the highest occupied (HOMO) and lowest unoccupied molecular (LUMO) orbitals of BDP molecular structure in gas via utilizing B3LYB/6-31G(d) level of theory.

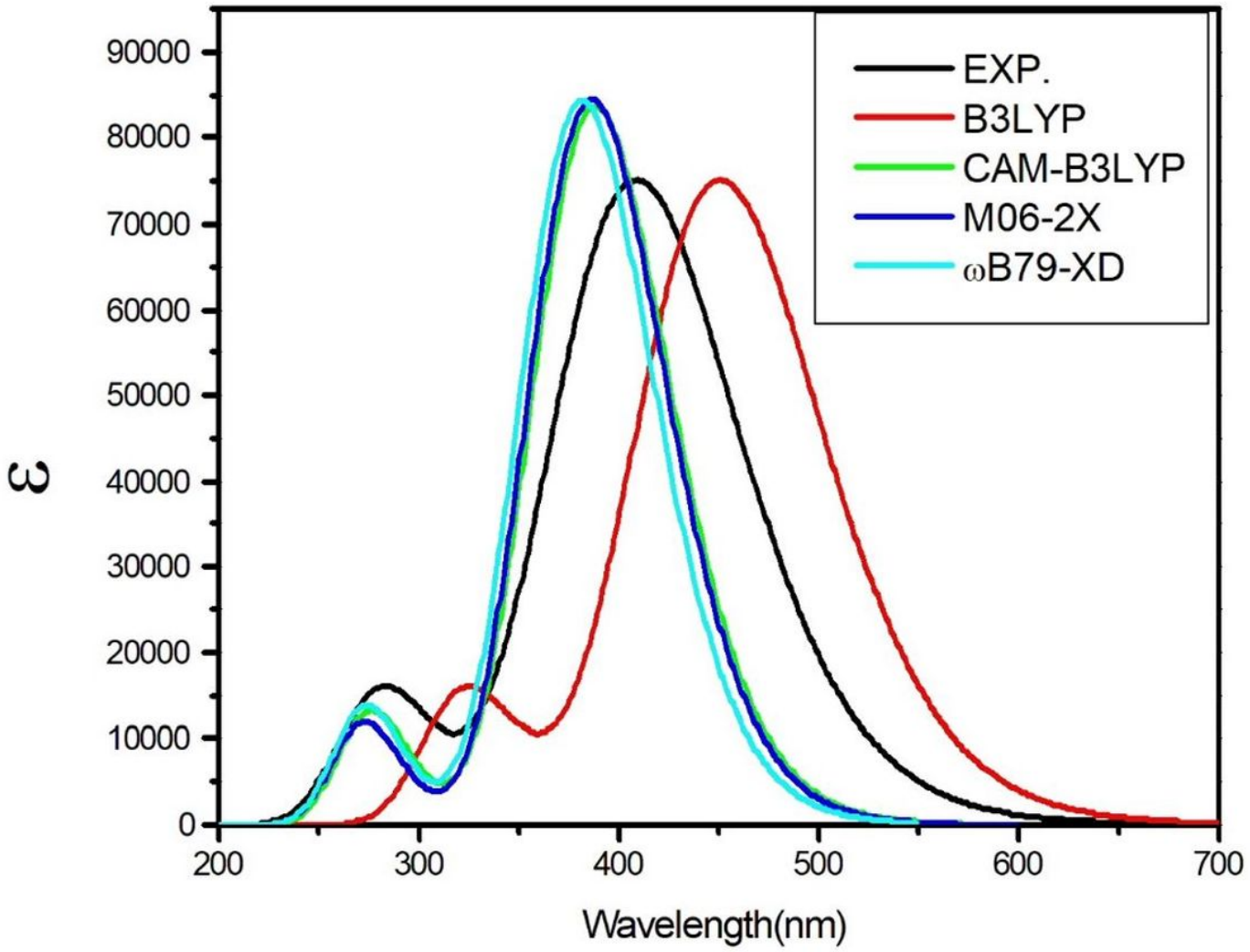

Figure 7

Calculated absorption spectra of BDP molecular structure given with the utilize of various functionals, B3LYP, CAMB3LYP, M06-2X and ωB97X-D and experimental absorption spectrum of the BDP (in black). Y-axis refers to calculated absorptivity. The 6-31G(d) basis set was satisfied.

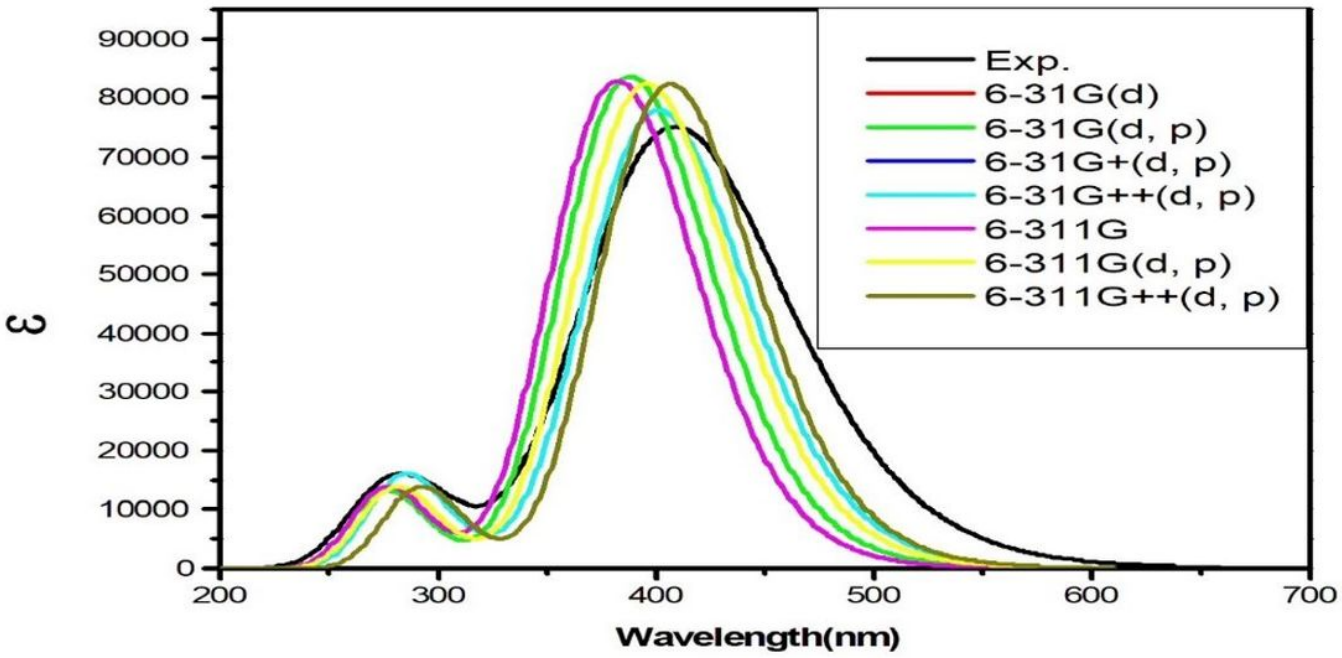

Figure 8

Calculated electronic absorption spectra of the BDP in ethanol with different basis sets and practical absorption spectrum (in black). Y-axis refers to calculated absorptivity. The CAM-B3LYP functional was applied.

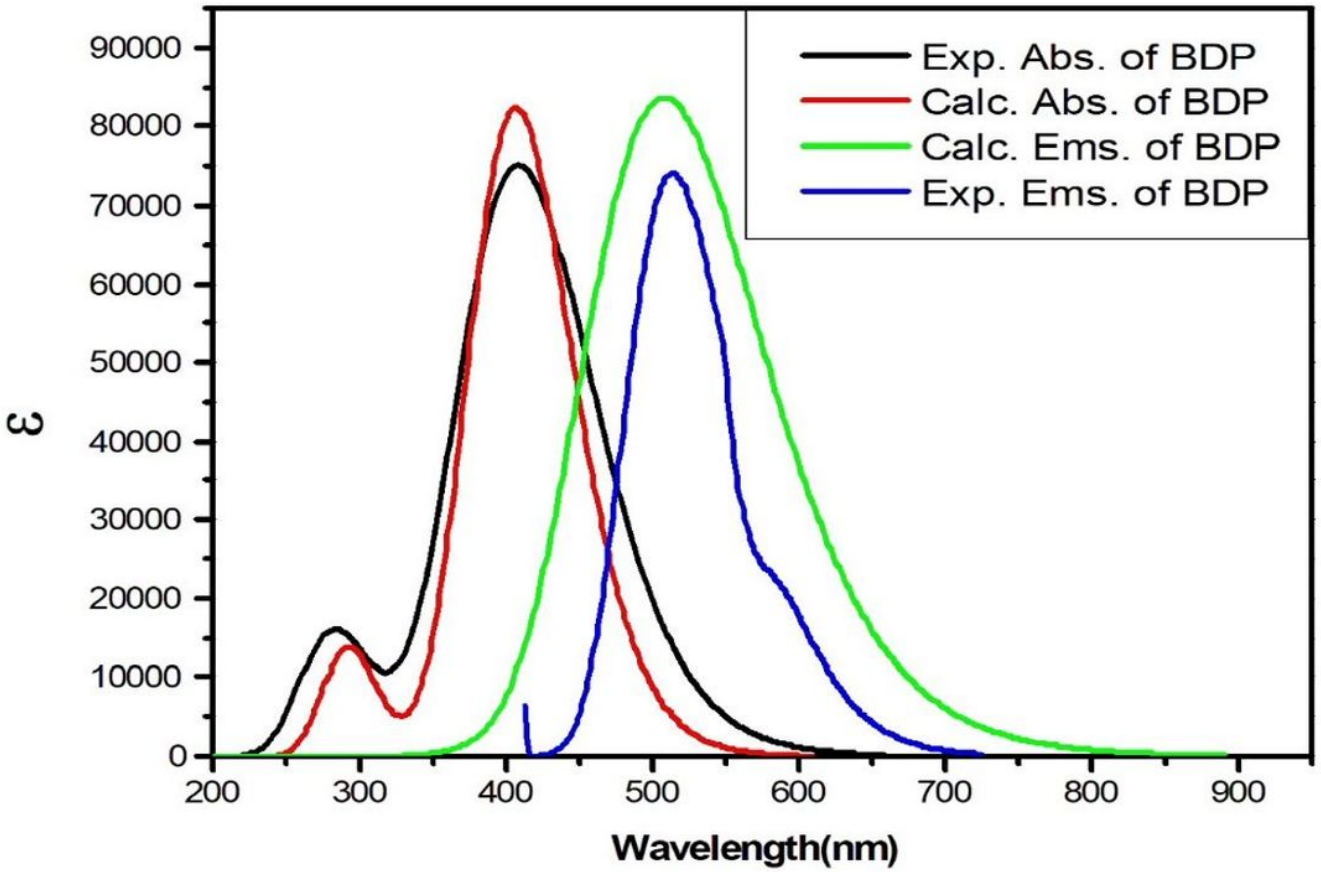

Figure 9

Calculated electronic absorption (Calc. Abs.) and emission spectra (Calc. Ems.) of the BDP in ethanol with different basis sets and experimental absorption (Exp. Abs.) and emission spectra (Exp. Ems.) of the BDP. Y- axis refers to calculated absorptivity. The CAM-B3LYP functional was applied with 6-311G++ (d, p) basis set.

Supplementary Files

This is a list of supplementary files associated with this preprint. Click to download.

- scheme1.jpg
- scheme2.jpg